ISBN: 978-3-95450-214-1 ISSN: 2673-5490 doi:10.18429/JACoW-IPAC2021-MOPAB102

CSR IMPEDANCE IN HEPS STORAGE RING*

Haisheng Xu†, Xiaoyu Li, Na Wang
Key Laboratory of Particle Acceleration Physics and Technology,
Institute of High Energy Physics, Chinese Academy of Sciences, Beijing, China

Abstract

High Energy Photon Source (HEPS) is under construction in Beijing, China. A quite complete impedance model was already built up in the preliminary design stage (named PDR version), based on the element-by-element impedance calculation. However, Coherent Synchrotron Radiation (CSR) impedance, which might affect the longitudinal collective effects, was not yet included in the PDR version impedance model. Therefore, we would like to compute the CSR impedance which was mainly generated at the bending magnets and the insertion devices. Both the latest design of HEPS storage ring lattice and the insertion devices were used in the calculations of the CSR impedance. The influence of the CSR impedance on the microwave instability threshold was also discussed.

INTRODUCTION

High energy photon source (HEPS) [1] is designed as a diffraction-limited storage ring (DLSR) based synchrotron light source, which is under construction in Beijing, China. The high quality (low emittance, high current, etc.) electron beam is the basis of the generation of high performance synchrotron light to the users. However, it's well known that the impedance induced collective effects, especially the collective beam instabilities, will degrade the beam quality significantly. Therefore, great efforts have been made to obtain the precise modeling of coupling impedance and to understand clearly the mechanism of the collective beam instabilities [2–4].

Both the resistive-wall and geometric impedance of the vacuum components were computed element by element for creating a relatively complete impedance model. Some very important impedance induced instabilities, such as the microwave instability, the transverse mode-coupling instability, and the coupled-bunch instabilities, were already evaluated based on the aforementioned impedance model in the preliminary design stage of HEPS.

However, the coherence synchrotron radiation (CSR) impedance, which was proven to be important sometimes in electron storage rings [5], hasn't been included in the impedance model yet. Even though the expected bunch length in the nominal design of HEPS storage ring was approximately hundreds picoseconds, which was quite long, the CSR impedance might still be worth to be computed and included in the total impedance model. The computation of CSR impedance was also suggested by the HEPS International Advisory Committee (IAC) during the second HEPS IAC meeting in 2019. The experiences of SLS-2 indicated that the CSR could have remarkable influences on the threshold of microwave instability [6]. This information also motivated us to compute and check the influences of the CSR impedance in HEPS storage ring.

Since CSR radiated mainly at the bending magnets and insertion devices, our computation of CSR impedance focused on these components. In the rest of this paper, we first review briefly the basic information of HEPS. Then, the computation of CSR impedance at bending magnets and insertion devices will be presented. The conclusions and discussions will be given afterwards.

BASIC INFORMATION OF HEPS

Recently, the HEPS lattice were updated to the v3.0, the main parameters of which were listed in Table 1, more detailed information about the v3.0 lattice could be found in [7].

Table 1: Main Lattice Parameters

Parameters	Symbols	Values and Units
Circumference	C	1 360.4 m
Beam Energy	E_0	6 GeV
Betatron Tunes	ν_x/ν_y	115.15 / 104.29
Chromaticity	C_x/C_y	+5 / +5
Momentum Compaction Factor	α_c	1.83e-5
Horizontal Damping Time	τ_x	10.86 ms
Vertical Damping Time	τ_y	20.62 ms
Longitudinal Damping Time	τ_δ	18.71 ms
Energy Loss per Turn w/o ID	U_0	2.64 MeV
RF Frequency	f_0	166.6 MHz
Harmonic Number	h	756

In the v3.0 lattice, the third harmonic cavities were also planned to be used for lengthening the bunches. The RMS bunch length under the ideal lengthening condition, without considering the impedance induced bunch lengthening, was about 100 ps. The corresponding cut-off frequency is approximately $f_{cut-off} \approx 3.4$ GHz. Therefore, the PDR version impedance model, truncated at about 38 GHz, was still enough in the v3.0 lattice situation.

* Work supported by National Natural Science Foundation of China (No. 11805217 and No. 11775239), the Youth Innovation Promotion Association CAS, NKPSTRD (2016YFA0402001)), and High Energy Photon Source (HEPS) project, a major national science and technology infrastructure in China.
† xuhs@ihep.ac.cn

ISBN: 978-3-95450-214-1 ISSN: 2673-5490 doi:10.18429/JACoW-IPAC2021-MOPAB102

CSR IMPEDANCE COMPUTATION

Generally speaking, the bending magnets and insertion devices were supposed to be the two types of the key components where CSR would radiate. We therefore carried out the computation of CSR impedance at the aforementioned two types of components.

Firstly, we focused on the computation of CSR impedance at bending magnets. The computation of CSR impedance was first carried out by assuming a point charge moving on a circle of radius R in free space, with the limit of $k \ll k_C = 3\gamma^3/(2R)$, using [8]

$$\left.\frac{Z_\parallel(k)}{L}\right|_{FS} = \frac{Z_0}{2\pi}\Gamma\left(\frac{2}{3}\right)\left(\frac{ik}{3R^2}\right)^{1/3}, \tag{1}$$

where $Z_0 \approx 120\pi$ represented the impedance of free space, L was the path length of the point charge.

However, the charges in an accelerator had to move in vacuum chambers, which were usually made by metallic materials with relatively small cross section. Previous work [9] indicated that shielding effects by the vacuum chambers might greatly affect the CSR impedance, meaning that the CSR impedance strongly depended on the boundary conditions of the vacuum chambers. The shielding effects could be considered by assuming to put two perfectly conducting parallel plates in the horizontal plane, the resulting formulae from which were written down using Bessel functions. However, this model was not easy to use in the numerical computations. Therefore, the simplified version represented by Airy functions, which was developed by D. M. Zhou in his Ph.D. Thesis [10], was used in this paper:

$$\begin{aligned}\left.\frac{Z_\parallel(k)}{L}\right|_{PP} = &\frac{2\pi Z_0}{b}\left(\frac{2}{kR}\right)^{1/3}\cdot \\ &\sum_{p=0}^{\infty}\left\{\mathrm{Ai}'\left(X_p^2\right)\left[\mathrm{Ai}'\left(X_p^2\right) - i\mathrm{Bi}'\left(X_p^2\right)\right]\right. \\ &\left.+X_p^2\mathrm{Ai}\left(X_p^2\right)\left[\mathrm{Ai}\left(X_p^2\right) - i\mathrm{Bi}\left(X_p^2\right)\right]\right\},\end{aligned} \tag{2}$$

where b represented the vertical aperture of the vacuum chamber of the bending magnet; R was the bending radius; Ai, Ai', Bi, Bi' were all Airy functions; X_p could be represented as follows

$$X_p = \frac{(2p+1)\pi}{b}\cdot\left(\frac{R}{2k^2}\right)^{1/3} \quad \text{for } p = 0, 1, 2, \cdots. \tag{3}$$

In HEPS storage ring, three different types of bending magnets, which were the longitudinal gradient bends (BLGs), the combined function bends (BDs) providing dipole and quadrupole magnetic fields simultaneously, and the anti-bends (ABs), were used. However, the models mentioned above were suitable only for the bends with constant magnetic field. Preprocessing and assumptions were therefore needed before the computations. In HEPS case, each BLG consists of five pieces with constant magnetic field at each piece. Therefore, the BLGs would be divided into 5 pieces in the computation of CSR impedance. The bending radius of the BDs and ABs were assumed to be constant in our computation. The used parameters of bending magnets in one 7BA cell were listed in Table 2.

Table 2: Bends' Parameters in One Cell of v3.0 Lattice

Indices	Length (m)	Angle (mrad)
ABF1	0.1800	-1.3406
ABF2	0.6100	-5.3770
ABF3	0.6100	-5.3770
ABF4	0.1800	-1.3406
BD1	1.0972	23.8688
BD2	1.0972	23.8688
BLG11	0.2998	7.2478
BLG12	0.2998	5.0291
BLG13	0.2998	4.2895
BLG14	0.2998	3.1062
BLG15	0.2998	1.9229
BLG21	0.2016	2.4668
BLG22	0.2016	2.7914
BLG23	0.2016	2.9212
BLG24	0.2016	3.2458
BLG25	0.2016	3.1809
BLG31	0.2043	5.2847
BLG32	0.2043	5.8131
BLG33	0.0400	1.9986
BLG34	0.2043	5.8131
BLG35	0.2043	5.2847
BLG41	0.2016	3.1809
BLG42	0.2016	3.2458
BLG43	0.2016	2.9212
BLG44	0.2016	2.7914
BLG45	0.2016	2.4668
BLG51	0.2998	1.9229
BLG52	0.2998	3.1062
BLG53	0.2998	4.2895
BLG54	0.2998	5.0291
BLG55	0.2998	7.2478

The aforementioned two widely accepted models, the free-space (FS) model and parallel-plates (PP) model, were both implemented in our computations. The resulting CSR impedance at bending magnets was shown in Fig. 1, where red curves and the blue curves stood for the real and imaginary parts of the CSR impedance, respectively. Solid curves represented the results obtained by using the FS model, while the dashed curves were obtained by the PP model (half gap 11 mm). It was clearly showing in Fig. 1 that CSR impedance below the frequency of 1e12 Hz was significantly suppressed by the vacuum chambers.

For the computation of CSR impedance in the insertion devices, the FS model developed in [11] was implemented. By converting from Gaussian Unit to SI Unit, the resulting formula became

$$Z(k) = \frac{1}{4}Z_0 L_w k\frac{k_w}{k_0}\left\{1 - \frac{2i}{\pi}\left[\log\left(\frac{4\mathrm{k}}{\mathrm{k}_0}\right) + \gamma_{\mathrm{E}}\right]\right\}, \tag{4}$$

where $\gamma_E \approx 0.5772$ was the Euler gamma constant.

ISBN: 978-3-95450-214-1 ISSN: 2673-5490 doi:10.18429/JACoW-IPAC2021-MOPAB102

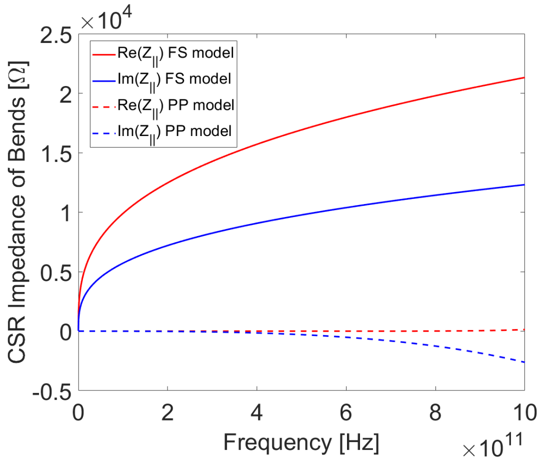

Figure 1: Total CSR impedance of bends using free space (FS) model (solid curves) and parallel plate (PP) model (dashed curves). The red curves and the blue curves stood for the real and imaginary parts of the CSR impedance, respectively.

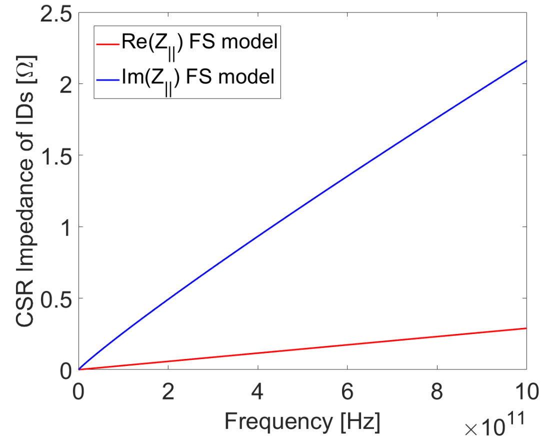

Figure 2: Total CSR impedance of main IDs (except APPLE-Knot undulator and MANGO wiggler) by using free space model.

In the Phase I of HEPS, two non-planar IDs, which were the APPLE-Knot undulator and the MANGO wiggler, would be used. However, the Eq. (4) was developed for the planar IDs only. Therefore, these two special non-planar IDs would not be included in the computations of this paper. The key parameters of the used IDs were listed in Table 3. The resulting first estimation of the CSR impedance induced by the Phase I IDs of HEPS were shown in Fig. 2.

Table 3: Main Parameters of the Used Phase I IDs

λ_w (m)	Length L_w (m)	K
0.0167	1.9539	1.8561
0.0226	3.9324	2.3219
0.012	1.968	0.9078
0.0142	1.9596	1.3263
0.0186	3.9618	1.8067
0.0199	3.9601	1.8029
0.0188	1.9552	2.3705
0.073	0.949	11.1818
0.05	0.816	6.6707
0.0228	1.938	2.5128
0.073	0.949	11.1818
0.035	4.935	2.8767
0.0327	4.9377	2.4433
0.025	4.975	1.2609
0.0327	4.6107	2.6877

CONCLUSIONS AND DISCUSSIONS

In this paper, the CSR impedance at bending magnets and Phase I IDs (except the two non-planar IDs) of HEPS storage ring v3.0 lattice was computed. As shown in Fig. 3, the computed CSR impedance was dramatically lower than the total impedance of all the vacuum components. Therefore, the CSR impedance shouldn't affect the beam performance of HEPS in the Phase I nominal operation.

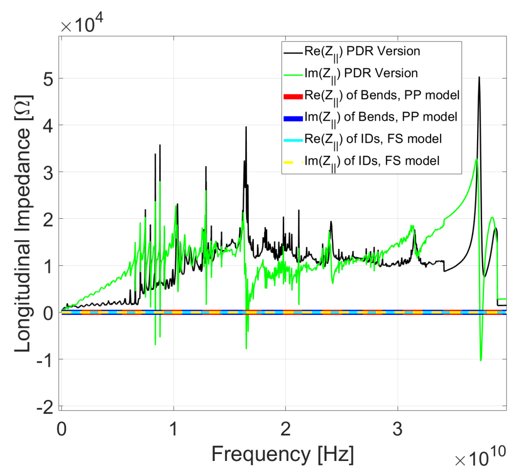

Figure 3: Comparison of the CSR impedance of bends (PP model), the CSR impedance of IDs and the PDR impedance model.

ACKNOWLEDGEMENT

The authors would like to thank the colleagues in the Accelerator Physics Group of IHEP for the fruitful discussions.

REFERENCES

[1] Yi Jiao *et al.*, "The HEPS project", *Journal of Synchrotron Radiation*, vol. 25, pp. 1611-1618, Nov. 2018. doi:10.1107/S1600577518012110

[2] N. Wang, Z. Duan, X. Y. Li, H. Shi, S. K. Tian, and G. Xu, "Development of the Impedance Model in HEPS", in *Proc. 8th Int. Particle Accelerator Conf. (IPAC'17)*, Copenhagen, Denmark, May 2017, pp. 3110–3113. doi:10.18429/JACoW-IPAC2017-WEPIK078

ISBN: 978-3-95450-214-1 ISSN: 2673-5490 doi:10.18429/JACoW-IPAC2021-MOPAB102

[3] N. Wang, Z. Duan, C. Li, S. K. Tian, and H. S. Xu, "Studies on Collective Instabilities in HEPS", in *Proc. 8th Int. Particle Accelerator Conf. (IPAC'17)*, Copenhagen, Denmark, May 2017, pp. 3763–3766. doi:10.18429/JACoW-IPAC2017-THPAB030

[4] N. Wang *et al.*, "Study of beam coupling impedance and beam collective effect in high energy photon source", *Atomic Energy Science and Technology*, vol. 53, pp. 1601-1606, 2019.

[5] K. L. F. Bane, Y. Cai, and G. Stupakov, "Threshold studies of the microwave instability in electron storage rings", *Phys. Rev. ST Accel. Beams*, vol. 13, p. 104402, Oct. 2020. doi:10.1103/PhysRevSTAB.13.104402

[6] M. M. Dehler, M. Aiba, A. Citterio, and L. Stingelin, "Overview of Collective Effects in SLS 2.0", in *Proc. 10th Int. Particle Accelerator Conf. (IPAC'19)*, Melbourne, Australia, May 2019, pp. 1658–1661. doi:10.18429/JACoW-IPAC2019-TUPGW107

[7] Y. Jiao *et al.*, "Progress of Lattice Design and Physics Studies on the High Energy Photon Source", presented at the 12th Int. Particle Accelerator Conf. (IPAC'21), Campinas, Brazil, May 2021, paper MOPAB053, this conference.

[8] A. Faltens and L. J. Laslett, "Longitudinal coupling impedance of a stationary electron ring in a cylindrical geometry", *Particle Accelerators*, vol. 4, pp. 151-157, 1973.

[9] J. S. Nodvick and D. S. Saxon, "Suppression of Coherent Radiation by Electrons in a Synchrotron", *Phys. Rev.*, vol. 96, pp. 180–184, Oct. 1954. doi:10.1103/PhysRev.96.180

[10] D. Zhou, "Coherent synchrotron radiation and microwave instability in electron storage ring", Ph.D. Thesis, Graduate University for Advanced Studies, Hayama, Japan, 2011.

[11] J. Wu, T. O. Raubenheimer, and G. V. Stupakov, "Calculation of the coherent synchrotron radiation impedance from a wiggler", *Phys. Rev. ST Accel. Beams*, vol. 6, p. 040701, Apr. 2003. doi:10.1103/PhysRevSTAB.6.040701